

# Distributed Predictive Control for Frequency and Voltage Regulation in Microgrids

Juan S. Gómez, Doris Sáez, *Senior Member, IEEE*, John W. Simpson-Porco, *Member, IEEE*,  
and Roberto Cárdenas, *Senior Member, IEEE*

**Abstract**—Distributed control schemes have transformed frequency and voltage regulation into a local task in distributed generators (DGs) rather than one central secondary controller. A distributed scheme is based on information shared among neighboring units; thus, the microgrid performance is affected by issues induced by the communication network. This paper presents a distributed predictive control applied to the secondary level on microgrids. The model used for prediction purposes is based on droop and power transfer equations, but communication features such as connectivity and latency are also included, thus making the controller tolerant to electrical and communication failures. The proposed controller considers as control objectives frequency and voltage regulation and consensus over the real and reactive power contributions from each power unit in the microgrid. The experimental results show that the proposed scheme (i) responds properly to load variations, working within operating constraints such as generation capacity and voltage range; (ii) preserves the control objectives when a power unit is disconnected and reconnected without any user updating in the controllers; and (iii) compensates the effects of communication issues over the microgrid dynamics.

**Index Terms**—Secondary Control, Distributed Predictive Control, Microgrids, Constrained Optimization, Plug and Play Controller.

## I. INTRODUCTION

MICROGRIDS are more sensitive than large-scale power systems to small changes in either load balance or power capacity. Currently, the microgrid community accepts as a fact that a distributed secondary control level is inherently fault tolerant to such electrical issues [1]. However, each controller in a distributed scheme should be able to calculate its control action according to its knowledge about the current state of the microgrid. The necessity of updating the microgrid knowledge implies good communication among the controllers; therefore, the communication performance and the microgrid performance are directly related.

In [2] and [3], information shared through the communication network updates an electrical model used by each secondary controller. This model is based on the microgrid admittance matrix, and it is applied to an optimization problem to achieve a stable operation point for frequency and voltage when any DG is either plugged in or unplugged. In this case, the electrical model is adjusted, without any user intervention, according to Kirchhoff's voltage law when some change occurs in the microgrid. This feature is called plug and play (PnP) capability.

A second approach to include the microgrid model at the secondary control level is a graph-based representation of the information flow among the DGs. In this case, the DGs are

represented as the graph vertices, and the communication links are represented as the graph edges. A weighted matrix that represents the graph connectivity among DGs is called the adjacency matrix. This matrix permits exploring the properties of the network systems [5]. In [4], a distributed consensus problem is applied over the microgrid. It is shown that the problem converges if and only if the microgrid graph has a path between any two DGs (connected graph), and the final value is the average of the initial conditions of the consensus variables.

One application of consensus in microgrids is the distributed averaging proportional-integral (DAPI) controller proposed in [6]. This scheme adds a term to the proportional-integral (PI) secondary controllers to achieve real power consensus for the frequency loop and reactive power consensus for the voltage loop. The DAPI controller is considered to be a PnP controller because the adjacency matrix can be updated online, and then the control law changes if a DG is connected to or disconnected from the microgrid. However, this controller is not robust against communication issues such as data dropouts or latency because its control law only considers current information.

Communication issues are not uncommon in networks because communication links are susceptible to external factors, such as weather, obstructions or interference. Data latency, data losses, and network topology changes are issues that generally degrade the control performance irrespective of what technology or topology is used in the network [8].

In [6], an updated adjacency matrix used by the DAPI controller permits confronting changes in the communication network topology, preserving the frequency and voltage regulation. In [9], latency effects in the frequency restoration loop are compensated by a PI controller with Smith predictor. To tune this, a constant delay estimation is used; however, the real delay in communication networks is not fixed. To solve this issue, in [10], a centralized PI controller with gain scheduling for frequency restoration is used to change the tuned point when the delay also changes.

A set of consensus-based controllers that ensure convergence for regulation and power sharing at a finite time have recently been reported. These PnP controllers have shown good performance against latency and communications path failures. In [11], two decoupled finite-time controllers that preserve the relations frequency-real power and voltage-reactive power are compared with a centralized controller using a six DG microgrid. Conversely, in [12], four independent finite-time controllers are used by each DG to regulate frequency

and voltage and to achieve real and reactive power sharing. The stability analysis of this scheme ensures convergence irrespective of the latency in the network.

Although predictive control is generally applied at the tertiary control level [14], its application to secondary control in microgrids is a promising approach because it is possible to confront data dropouts and latency. In [9], a centralized predictive controller is implemented to regulate the frequency in a microgrid with two DGs, showing a better latency compensation than the Smith predictor. Furthermore, if predictive control is combined with a distributed scheme, it is possible to include PnP capability [16]. The challenge to implement predictive controllers at the secondary level of microgrids is defining an optimization problem that is able to be solved in a short sampling period.

In a distributed model-based predictive control (DMPC) scheme, a (discrete-time) system model is used by each controller to predict its self-behavior over a prediction horizon. The used model is based on local information (i.e., measurements) and shared information from other controllers (i.e., previously computed predictions), and it is introduced as a set of equality constraints into an optimization problem. The system solution minimizes a cost function based on the predicted trajectory and the information exchanged with other DGs. Although the optimal solution provides a sequence of control actions, only the first element is applied, and the optimization problem is solved again at the next sampling period (rolling horizon scheme) [20].

There are two methods to solve the DMPC. The iterative method optimizes and shares the result with other DMPCs several times within the time step. The noniterative method optimizes only once per time step to reduce the traffic over the communication network [19].

Three iterative DMPC schemes for frequency regulation in large-scale power systems are proposed in [21]. The model used for these controllers is based on the frequency-active power relationship, and these are compared with an automatic generation controller (AGC) and a centralized MPC (CMPC) over a communication network with the same topology as the electrical system. Because these are iterative schemes, they require considerable computational effort and a high-performance communication network; therefore, the implementation of these predictive controllers is expensive for actual microgrids.

In [22], an unconstrained DMPC, which include consensus, is proposed for voltage regulation in microgrids, whereas the frequency regulation is achieved using a DAPI controller. In this scheme, an analytical solution is achieved for voltage regulation, reducing the computational effort.

#### A. Paper Contributions

As it was shown, the PnP schemes using consensus techniques in addition to the regulation task (frequency and/or voltage) enable improving the microgrid secondary level performance in several scenarios. However, we consider that the predictive control has not been completely exploited for these applications. In this paper, we propose a noniterative DMPC

that is capable of real-time operation in environments with communications issues, preserving the PnP capability.

The main advantage of our controller is the model used to predict the microgrid behavior. This model is based on local voltage, frequency and power equations, and it includes a communication network model that also represents connectivity and latency. The local model on each controller is updated once per sampling period with local measurements over each DG and with information shared from neighboring DGs. The model permits including explicit operational constraints, such as voltage range and apparent power limits. Experimental results over a three DG microgrid validate the good performance of the proposed controller.

This paper is organized as follows. In Section II, the framework of the model used to build the optimization problem is presented. In Section III, the optimization problem used in the DMPC is detailed. The features of and parameters used in the experimental setup, as well as the obtained results, are shown in Section IV. The paper conclusions and final remarks are presented in Section V.

## II. MODEL USED FOR CONTROL DESIGN

Considering that variables such as frequency, voltage, and real and reactive power are coupled in microgrids, the proposed model reflects this behavior based on droop, power transfer and phase angle equations. Additionally, a communication network model that considers the latency, defined by delay terms ( $z^{-\tau_{ij}}$ ), and the connectivity, defined by adjacency terms ( $a_{ij}$ ), is also proposed.

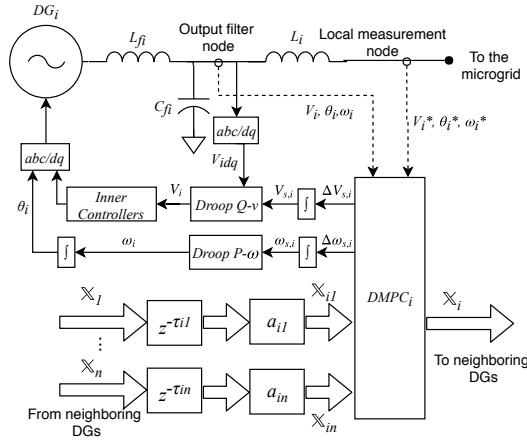
Because the model computes the power contribution of DG<sub>*i*</sub> to the microgrid, external measurements are required. Voltage, frequency and phase angle are measured/estimated at the *LC* filter output ( $V_i, \omega_i, \theta_i$ ) and at an adjacent measurement node ( $V_i^*, \omega_i^*, \theta_i^*$ ). This adjacent measurement node is defined as the downstream node to the coupling inductance  $L_{ij}$ .

The control scheme for DG<sub>*i*</sub> in the microgrid is shown in Fig. 1. Note that the inner and droop controllers (primary level) work on a *dq* framework, whereas  $\omega_{s,i}$  and  $V_{s,i}$  signals are droop inputs that compensate voltage and frequency deviations. These signals and  $\mathbb{X}_i$  are from the proposed DMPC (secondary level), and these are computed as a solution to an optimization problem.  $\mathbb{X}_i$  is composed by frequency, voltage and power predictions, and it is shared with neighboring DGs using the communication network.

A description of each equation used to build the proposed model is included below, and the optimization problem and  $\mathbb{X}_i$  will be defined in Section III.

#### A. Droop Equations

Droop control provides statism to the microgrid, changing the operating point from the nominal frequency/voltage to ensure the real/reactive power supply when the microgrid is disturbed. The droop control laws (1) and (2) define the linear relations frequency-real power and voltage-reactive power, respectively, where  $\omega_0$  and  $V_0$  represent the nominal frequency and voltage,  $M_{p\omega,i}$  and  $M_{qv,i}$  are the droop slopes, and  $\omega_{s,i}$  and  $V_{s,i}$  are the secondary control actions for unit *i*.

Fig. 1. DMPC<sub>*i*</sub> Diagram.

Droop equations are included in the secondary control model because they determine the joint point between the primary and secondary control levels.

$$\omega_i(t) = \omega_0 + M_{p\omega,i} P_i(t) + \omega_{s,i}(t) \quad (1)$$

$$V_i(t) = V_0 + M_{qv,i} Q_i(t) + V_{s,i}(t) \quad (2)$$

### B. Phase Angle Equation

The phase angle deviation ( $\delta\theta_i$ ) generated for unit  $i$  by the coupling inductance  $L_i$  is defined by (3). The coupling inductance is a common passive element used to connect the low-pass filter output to the microgrid. For our controller, the phase angle deviation is required for estimating the real/reactive power transferred from the DG to the microgrid. To estimate  $\delta\theta_i(t)$  properly, phase-locked loops (PLLs) should be placed at the output filter and the adjacent measurement node.

$$\delta\theta_i(t) = \theta_i(t) - \theta_i^*(t) = \int_0^t [\omega_i(\tau) - \omega_i^*(\tau)] d\tau \quad (3)$$

### C. Power Transfer Equations

To achieve power consensus in the microgrid, it is necessary to estimate the power contribution of each DG in the microgrid. In this case, our controller neglects the use of an admittance matrix-based model, as is generally used, to propose a model based on the power transferred through the coupling inductance. The equations that determine the power transferred from unit  $i$  to the microgrid are defined in (4) and (5), where  $B_i = 1/L_i\omega_0$ .

$$P_i(t) = B_i V_i(t) V_i^*(t) \sin(\delta\theta_i(t)) \quad (4)$$

$$Q_i(t) = B_i [V_i(t)^2 - V_i(t) V_i^*(t) \cos(\delta\theta_i(t))] \quad (5)$$

### D. Discrete Time Model

Before deriving a predictive model, equations (1) to (5) are discretized using the forward Euler method, where  $t_n = nT_{sec}$ ,  $n \in \mathbb{Z}^+$ , and  $T_{sec}$  is the sampling period used at the secondary control level. To eliminate the steady-state error, integrators are added at the DMPC outputs; therefore, the

incremental operator  $\Delta$ , defined by (??), is applied on (1) and (2) to compute  $\Delta\omega_{s,i}$  and  $\Delta V_{s,i}$ .

$$\Delta f(t_n) = [f(t_n) - f(t_{n-1})] \quad (6)$$

Additionally Taylor expansion is applied to (4) and (5) around the measured/estimated point  $\{\omega_i(t_n), \omega_i^*(t_n), V_i(t_n), V_i^*(t_n), \delta\theta_i(t_n), P_i(t_n), Q_i(t_n)\}$ , simplifying the optimization problem. The linear and discrete time model is shown in (6).

$$\omega_i(t_{n+1}) = \omega_i(t_n) + M_{p\omega,i} [P_i(t_{n+1}) - P_i(t_n)] + \Delta\omega_{s,i}(t_n) \quad (7a)$$

$$V_i(t_{n+1}) = V_i(t_n) + M_{qv,i} [Q_i(t_{n+1}) - Q_i(t_n)] + \Delta V_{s,i}(t_n) \quad (7b)$$

$$\delta\theta_i(t_{n+1}) = \delta\theta_i(t_n) + T_{sec} [\omega_i(t_{n+1}) - \omega_i^*(t_n)] \quad (7c)$$

$$P_i(t_{n+1}) = P_i(t_n) + [V_i(t_{n+1}) - V_i(t_n)] B_i V_i^*(t_n) \sin(\delta\theta_i(t_n)) + [\delta\theta_i(t_{n+1}) - \delta\theta_i(t_n)] B_i V_i(t_n) V_i^*(t_n) \cos(\delta\theta_i(t_n)) \quad (7d)$$

$$Q_i(t_{n+1}) = Q_i(t_n) + [V_i(t_{n+1}) - V_i(t_n)] B_i [2V_i(t_n) - V_i^*(t_n) \cos(\delta\theta_i(t_n))] + [\delta\theta_i(t_{n+1}) - \delta\theta_i(t_n)] B_i V_i(t_n) V_i^*(t_n) \sin(\delta\theta_i(t_n)) \quad (7e)$$

### E. Communication Network Model

In this work, a full-duplex communication network is considered in which the bidirectional link between units  $i$  and  $j$  is represented by an adjacency term  $a_{ij}$  and a delay term  $\tau_{ij}$ . The adjacency term represents the connectivity between two units and is defined as (7). This term is updated at the beginning of each sampling period according to the information received in unit  $i$ .

$$a_{ij}(t_n) = \begin{cases} 1 & \text{Data from unit } j \text{ arrives to unit } i \text{ at } t_n \\ 0 & \text{Data from unit } j \text{ does not arrive to unit } i \text{ at } t_n \\ 0 & j = i \end{cases} \quad (8)$$

The delay term ( $\tau_{ij} \geq 1$ ) is measured in sampling periods, and it represents the time required for the transmission-reception process between DG<sub>*i*</sub> and DG<sub>*j*</sub>. Since the communication is full duplex, the associated graph is undirected; then, the equalities  $\tau_{ij} = \tau_{ji}$  and  $a_{ij} = a_{ji}$  are satisfied.

## III. OPTIMIZATION FOR PREDICTIVE CONTROL

Predictive control optimizes a cost function using a set of equalities and inequalities as constraints that reflect the system behavior. The cost function and the constraints should be functions of the predicted variables. The optimal solution is a vector  $\mathbb{X}$  that contains the predicted values over the prediction horizon  $N_y$  and the control sequence over the control horizon  $N_u$ . For our controller, it is possible to use the set of equations (6) to predict the DG behavior. Because controlled variables are explicit in the predictive model, it is possible to directly include operational constraints. The optimization problem and how it is solved are detailed below.

### A. Predictive Model

The set of equations (6) can be used to determine the DG behavior at  $t_{n+k}$ , where  $k \in \mathbb{Z}^+$ . Considering the linearization of (6d) and (6e) around the measured point at  $t_n$ , their coefficients are updated each sampling period and assumed to be constants through the prediction horizon in the optimization problem.

$$\omega_i(t_{n+k}) = \omega_i(t_{n+k-1}) + M_{p\omega,i} [P_i(t_{n+k}) - P_i(t_{n+k-1})] + \Delta\omega_{s,i}(t_{n+k-1}) \quad (9a)$$

$$V_i(t_{n+k}) = V_i(t_{n+k-1}) + M_{qv,i} [Q_i(t_{n+k}) - Q_i(t_{n+k-1})] + \Delta V_{s,i}(t_{n+k-1}) \quad (9b)$$

$$\delta\theta_i(t_{n+k}) = \delta\theta_i(t_{n+k-1}) + T_{sec} [\omega_i(t_{n+k}) - \omega^*(t_n)] \quad (9c)$$

$$P_i(t_{n+k}) = P_i(t_n) + [V_i(t_{n+k}) - V_i(t_n)] B_i V_i^*(t_n) \sin(\delta\theta_i(t_n)) + [\delta\theta_i(t_{n+k}) - \delta\theta_i(t_n)] B_i V_i(t_n) V_i^*(t_n) \cos(\delta\theta_i(t_n)) \quad (9d)$$

$$Q_i(t_{n+k}) = Q_i(t_n) + [V_i(t_{n+k}) - V_i(t_n)] B_i [2V_i(t_n) - V_i^*(t_n) \cos(\delta\theta_i(t_n))] + [\delta\theta_i(t_{n+k}) - \delta\theta_i(t_n)] B_i V_i(t_n) V_i^*(t_n) \sin(\delta\theta_i(t_n)) \quad (9e)$$

### B. Operational Constraints

The set of operational constraints is composed of equalities and inequalities included to ensure the DG performance within the physical limits. This set of constraints is defined in (9).

$$\bar{\omega}_i(t_{n+k}) = \frac{\omega_i(t_{n+k}) + \sum_{j=1}^n a_{ij}(t_n) \omega_j(t_{n+k-\hat{\tau}_{ij}})}{1 + \sum_{j=1}^n a_{ij}(t_n)} \quad (10a)$$

$$\bar{V}_i(t_{n+k}) = \frac{V_i(t_{n+k}) + \sum_{j=1}^n a_{ij}(t_n) V_j(t_{n+k-\hat{\tau}_{ij}})}{1 + \sum_{j=1}^n a_{ij}(t_n)} \quad (10b)$$

$$\bar{\omega}_i(t_{n+N_y}) = \omega_0 \quad (10c)$$

$$\bar{V}_i(t_{n+N_y}) = V_0 \quad (10d)$$

$$\bar{V}_{\min} \leq \bar{V}_i(t_{n+k}) \leq \bar{V}_{\max} \quad (10e)$$

$$|P_i(t_n)| + |Q_i(t_n)| + \text{sign}(P_i(t_n)) [P_i(t_{n+k}) - P_i(t_n)] + \text{sign}(Q_i(t_n)) [Q_i(t_{n+k}) - Q_i(t_n)] \leq S_{\max} \quad (10f)$$

Note that equations (9a) and (9b), which define the frequency and voltage averages, include the parameters  $a_{ij}$  and  $\hat{\tau}_{ij}$ . Therefore,  $a_{ij}$  forces including only the received information to estimate and predict the averages, providing robustness against communication path failures and data losses.  $\hat{\tau}_{ij}$  represents the delay estimation in the communication process for compensating the network latency over the predicted averages.

Equations (9c) and (9d) force the average values to converge at the end of the prediction horizon  $N_y$ . Additionally, inequalities (9e) and (9f) ensure that the average voltage in the microgrid and the apparent power of DG<sub>*i*</sub> remain within a specific range. Inequality (9f) is defined as a polytopic inner approximation of (10) using the triangular inequality.

$$|S_i(t)| = (P_i(t)^2 + Q_i(t)^2)^{1/2} < S_{\max} \quad (11)$$

### C. Cost Function

The cost function (11) is built from six weighted terms, where each one represents a control objective in the microgrid. The first two terms represent the average frequency and average voltage regulation. Although the optimization problem is local for each DG, the regulation is global over the entire microgrid because these terms are based on predictions shared through the communication network. The third and fourth terms minimize the control action required by DG<sub>*i*</sub> to achieve the control objectives. The last two terms find a consensus over the contribution of real and reactive power for neighboring DGs.

$$J_i(t_n) = \sum_{k=1}^{N_y} [\lambda_{1i} (\bar{\omega}_i(t_{n+k}) - \omega_0)^2 + \lambda_{2i} (\bar{V}_i(t_{n+k}) - V_0)^2] + \sum_{k=1}^{N_u} [\lambda_{3i} (\Delta\omega_{s,i}(t_{n+k-1}))^2 + \lambda_{4i} (\Delta V_{s,i}(t_{n+k-1}))^2] + \sum_{j=1, j \neq i}^n \sum_{k=1}^{N_y} \lambda_{5i} a_{ij}(t_n) \left( \frac{P_i(t_{n+k})}{|S_i \max|} - \frac{P_j(t_{n+k-\hat{\tau}_{ij}})}{|S_j \max|} \right)^2 + \sum_{j=1, j \neq i}^n \sum_{k=1}^{N_y} \lambda_{6i} a_{ij}(t_n) \left( \frac{Q_i(t_{n+k})}{|S_i \max|} - \frac{Q_j(t_{n+k-\hat{\tau}_{ij}})}{|S_j \max|} \right)^2 \quad (12)$$

### D. Quadratic Programming Formulation

It is possible to build a quadratic programming (QP) problem for each DG in the microgrid, as is defined in (??), where matrices/vectors  $H_i, F_i, A_i, B_i, A_{eq,i}, B_{eq,i}$  are built from (8), (9) and (11). Then, the output vector  $\mathbb{X}_i$  is defined by (??), where the set of predicted variables is represented by  $\mathbb{X}_{p,i}$  and the predicted control sequences  $\mathbb{X}_{\Delta,i}$  are defined by (??) and (??), respectively.

$$\begin{aligned} \underset{\mathbb{X}_i}{\text{minimize}} \quad & J_i(t_n) := \frac{1}{2} \mathbb{X}_i^T H_i \mathbb{X}_i + F_i^T \mathbb{X}_i \\ \text{subject to} \quad & A_i \mathbb{X}_i \leq B_i \end{aligned} \quad (13)$$

$$A_{eq,i} \mathbb{X}_i = B_{eq,i} \quad (14)$$

$$\mathbb{X}_i = \{\mathbb{X}_{p,i}, \mathbb{X}_{\Delta,i}\} \quad (14)$$

$$\mathbb{X}_{p,i} = \{\bar{\omega}_i(t_{n+k}), \bar{V}_i(t_{n+k}), \omega_i(t_{n+k}), V_i(t_{n+k}), \delta\theta_i(t_{n+k}), P_i(t_{n+k}), Q_i(t_{n+k})\}_{k=1}^{N_y} \quad (15)$$

$$\mathbb{X}_{\Delta,i} = \{\Delta\omega_{s,i}(t_{n+k}), \Delta V_{s,i}(t_{n+k})\}_{k=1}^{N_u} \quad (16)$$

As mentioned in [20], a stable predictive control requires a feasible solution to the optimization problem. Note that (9c) to (9f) are related to the QP feasibility, ensuring that the system operates within physical limits over the whole prediction horizon. To ensure a feasible initial condition, the DMPC is enabled when the microgrid is operating at  $\omega_0$  and  $V_0$ . In a black start scenario, this state is achieved when the primary control level operates without load.

The computational cost is also related to the QP feasibility. Range and final value constraints limit the feasible solution space of the QP problem; then, the computational cost to solve it is also reduced [20]. In this case, we use the QPKWIK algorithm to solve the QP problem (??), which is an efficient and stable variation of the classic active-set method [26].

## IV. EXPERIMENTAL SETUP AND RESULTS

### A. Experimental Setup

To validate the proposed DMPC strategy, an experimental setup was built in the Microgrids Control Lab. of the University of Chile. The setup uses PM15F120 and PM5F60 *Triphase*® modules to emulate a three DG microgrid. Each module is controlled by a real-time target (RTT) computer, where the DMPC for each DG is downloaded. External measurement devices were connected to the measurement nodes, and these have direct communication with their respective RTTs. A diagram of the setup is shown in Fig. 2, and a photo register is shown in Fig. 3. In Table I and Table II, electrical and droop parameters are presented.

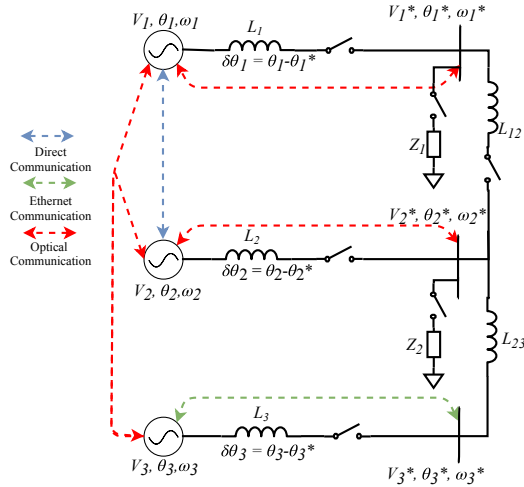


Fig. 2. Experimental Microgrid Diagram.

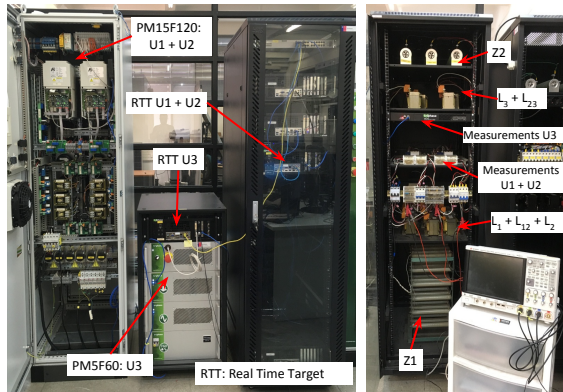


Fig. 3. Experimental Setup.

TABLE I  
MICROGRID ELECTRICAL PARAMETERS

Parameter	Description	Value
$T_{prim}$	Primary Level Sampling Period	1/16E3 s
$Z_1$	Load 1	11 $\Omega$
$Z_2$	Load 2	22 $\Omega$
$L_i$	Coupling Inductance	2.5 mH
$L_{ij}$	Transmission Line Inductance	2.5 mH
$\omega_0$	Nominal Frequency	314.159 rad/s
$V_0$	Nominal Voltage (peak)	150 V
$\omega_c$	Cutoff Frequency - Droop Controller	2 $\pi$ rad/s

TABLE II  
POWER CAPACITIES AND DROOP SLOPES

Power Capacities and Droop Slopes		DG <sub>1</sub>	DG <sub>2</sub>	DG <sub>3</sub>
$S_{max}$ [KVA]	Power Capacity	2.4	1.92	1.2
$M_{p\omega}$ [ $\frac{\text{rad}}{\text{sW}}$ ]	P- $\omega$ Droop Slope	-1E-4	-1.5E-4	-2.5E-4
$M_{qv}$ [ $\frac{\text{V}}{\text{VAR}}$ ]	Q-V Droop Slope	-1E-3	-1.5E-3	-1.8E-3

The weighting factors used in the cost function allow managing the tradeoff among the control objectives, and if required, giving priority to one of the control objectives over the other ones. In Table III and Table IV, the DMPC general parameters and weighting factors are shown. PI inner loops gains and other parameters that are not relevant to DMPC are omitted in this paper.

TABLE III  
DMPC GENERAL PARAMETERS

Parameter	Description	Value
$T_{sec}$	Secondary Level Sampling Period	0.05 s
$\tau_{ij}$	Estimated Communication Delay	0.05 s
$N_y$	Prediction Horizon	10
$N_u$	Control Horizon	10
$V_{max}$	Maximum Voltage	155V
$V_{min}$	Minimum Voltage	145V

TABLE IV  
DMPC WEIGHTING FACTORS

Weighting Factors		DG <sub>1</sub>	DG <sub>2</sub>	DG <sub>3</sub>
$\lambda_1$ [ $\frac{\text{s}}{\text{rad}}$ ] <sup>2</sup>	Average Frequency Error	3E4	5E4	9E4
$\lambda_2$ [ $\frac{1}{\text{V}}$ ] <sup>2</sup>	Average Voltage Error	5E0	6E0	7E0
$\lambda_3$ [ $\frac{\text{s}}{\text{rad}}$ ] <sup>2</sup>	Frequency Control Action	8E4	8E4	9E5
$\lambda_4$ [ $\frac{1}{\text{V}}$ ] <sup>2</sup>	Voltage Control Action	5E3	5E3	5E3
$\lambda_5$ [ $\frac{\text{VA}}{\text{W}}$ ] <sup>2</sup>	Real Power Consensus	1.5E2	1.3E2	2E2
$\lambda_6$ [ $\frac{\text{VA}}{\text{VAR}}$ ] <sup>2</sup>	Reactive Power Consensus	5E3	2E3	1E3

Four scenarios were implemented with the experimental setup using the proposed DMPC. The first (base case) scenario shows the DMPC performance when the microgrid is disturbed with load changes. In the second scenario, a communication failure between DG<sub>1</sub> and DG<sub>2</sub> is forced while the microgrid is disturbed. The third scenario is a PnP test, where DG<sub>3</sub> is disconnected and reconnected to the microgrid. Finally, the fourth scenario shows the microgrid performance when the latency changes over the communication network.

### B. Test Scenario 1 (Base Case)- Load Changes

This scenario tests the microgrid behavior using the proposed DMPC when several load changes are applied. In this case, the microgrid begins without load, and at  $t = 38\text{s}$ , load  $Z_1$  is connected to the microgrid; at  $t = 58\text{s}$ , the total load in the microgrid is composed of  $Z_1$  and  $Z_2$ ; and at  $t = 78\text{s}$  and  $t = 98\text{s}$ , the load is reduced to  $Z_1$  and zero, respectively.

In Fig. 4 and Fig. 6, it is shown that the average frequency and average voltage are regulated; however, voltage deviations over each DG caused by the microgrid heterogeneity are observed. Fig. 5 and Fig. 7 show that the consensus of real

and reactive power are achieved. In these figures, the power contribution of each DG is normalized with respect to its capacity.

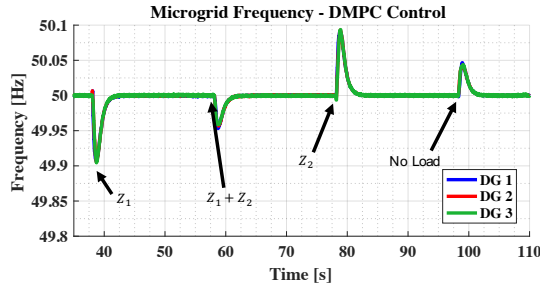


Fig. 4. Frequency Regulation Against Load Changes - DMPC Base Case.

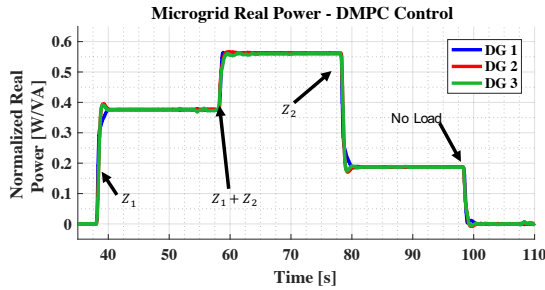


Fig. 5. Real Power Consensus Against Load Changes - DMPC Base Case.

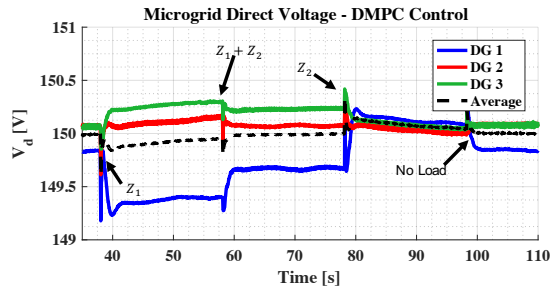


Fig. 6. Voltage Regulation Against Load Changes - DMPC Base Case.

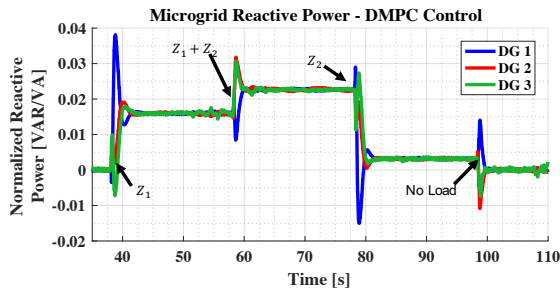


Fig. 7. Reactive Power Consensus Against Load Changes - DMPC Base Case.

Over the whole test, the microgrid is preserved as in Fig. 2, and the disturbances are limited to load changes. In this case, the adjacency matrix is constant and given by (12).

$$A(t) = \begin{bmatrix} a_{11} & a_{12} & a_{13} \\ a_{21} & a_{22} & a_{23} \\ a_{31} & a_{32} & a_{33} \end{bmatrix} = \begin{bmatrix} 0 & 1 & 1 \\ 1 & 0 & 1 \\ 1 & 1 & 0 \end{bmatrix} \quad (17)$$

This test scenario shows the basic microgrid operation, and it is considered as a base case for comparisons with the next scenarios tested in this paper.

### C. Test Scenario 2 - Communication Path Failure

This scenario adds to the base case a failure over the communication path between DG<sub>1</sub> and DG<sub>2</sub> at  $t = 50$ s. This failure is kept until the end of the test. This type of failure can be understood as a physical failure over the communication path or a simple data packet loss. In this case, as the adjacency matrix is a function of the information received for each controller, it is updated when the communication fails, preserving the average values.

The microgrid response is shown in Fig. 8. From the results, it is possible to state that the microgrid remains stable, achieving the four control objectives (frequency/voltage regulation and real/reactive power consensus) even when the communication path fails, it can be understood as a communication fault tolerance feature of the proposed DMPC; however, as shown in Fig. 9, a difference in the transient state is observed when load changes are applied. This change is caused by the relationship between the adjacency matrix and the cost function (11); as the adjacency terms are updated, but not the weighting factors, the tuned parameters do not compensate the load changes as when the communication network is complete.

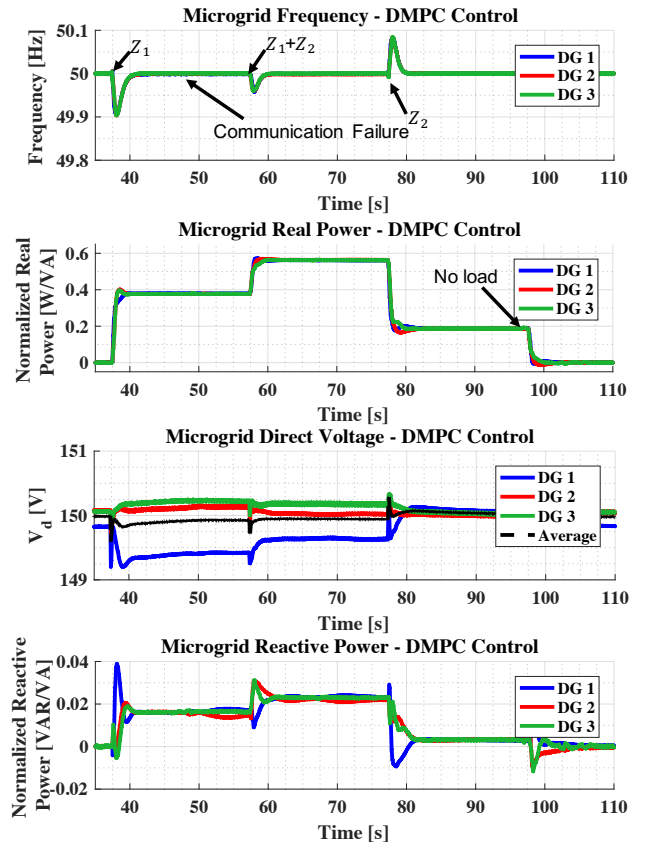


Fig. 8. Microgrid Response Against Communication Failure Between DG<sub>1</sub> and DG<sub>2</sub>.

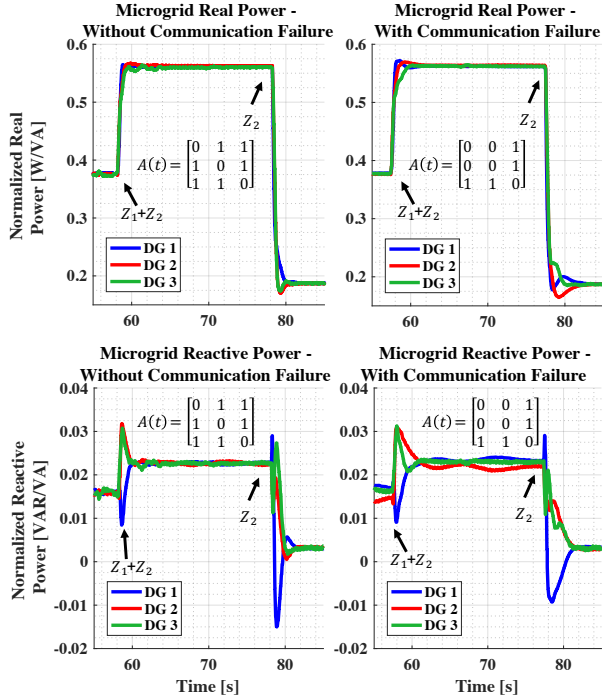


Fig. 9. Consensus Detail - Microgrid Response Against Communication Failure Between  $DG_1$  and  $DG_2$ .

#### D. Test Scenario 3 - Plug and Play Capability

This test shows the microgrid response when  $DG_3$  fails and it is disconnected (at  $t \approx 49s$ ), and after a synchronization sequence, it is reconnected to the microgrid (at  $t \approx 75s$ ). When  $DG_3$  is disconnected from the microgrid, its secondary control is disabled, and after the reconnection, it is enabled again. Fig. ?? shows a power distribution according to the DGs connected to the microgrid. Because the adjacency matrix  $A(t)$  depends on the information received by each DG, it is updated when  $DG_3$  is disconnected and reconnected, adjusting the consensus and the average values in the optimization problem. Between  $t \approx 75s$  and  $t \approx 78s$ , the real and reactive power contributions of  $DG_3$  are not in consensus even though it is connected to the microgrid. In this period,  $DG_3$  is synchronized ( $\delta\theta_3 = 0$ ), and its secondary controller is disabled; then, according to (4) and (5), only the reactive power flow through  $L_3$  is feasible. When the secondary controller is enabled on  $DG_3$ , the power consensus among the three units is re-established.

#### E. Test Scenario 4 - Communication Delay Response

This scenario compares the microgrid response at different values of  $\tau_{ij}$  but preserving  $\hat{\tau}_{ij}$  at one sampling period (0.05s). For each test, the same load changes from scenario 1 are applied. The results for frequency regulation and real power consensus are shown in Fig. ?? and Fig. ??, respectively. From the results, it is possible to state that the microgrid response increases its overshoot and its settling time when the communication delay also increases; however, the microgrid achieves the control objectives even when the delay is twenty times the sampling period ( $T_{sec}$ ).

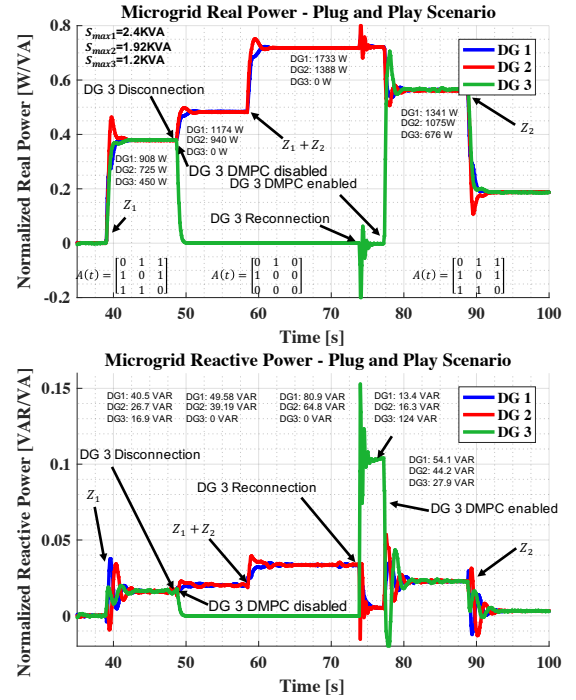


Fig. 10. Real Power (top) and Reactive Power (bottom) Behavior - Plug and Play Test

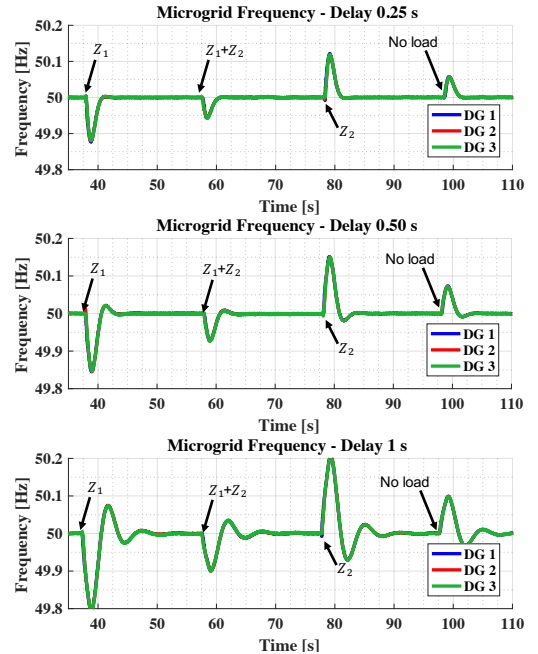


Fig. 11. Microgrid Behavior with Communication Delays- Frequency response- top: $\tau_{ij} = 0.25s$  middle: $\tau_{ij} = 0.5s$  bottom: $\tau_{ij} = 1s$

The DMPC latency compensation is related to the rolling prediction/control horizons, the sampling period and the delay estimation  $\hat{\tau}_{ij}$ ; however, either longer horizons or a shorter sampling period increase the computational effort. Even when the optimization problem is solved based on delayed information from neighboring DGs, the rolling horizon scheme updates the control sequence each sampling period, compen-

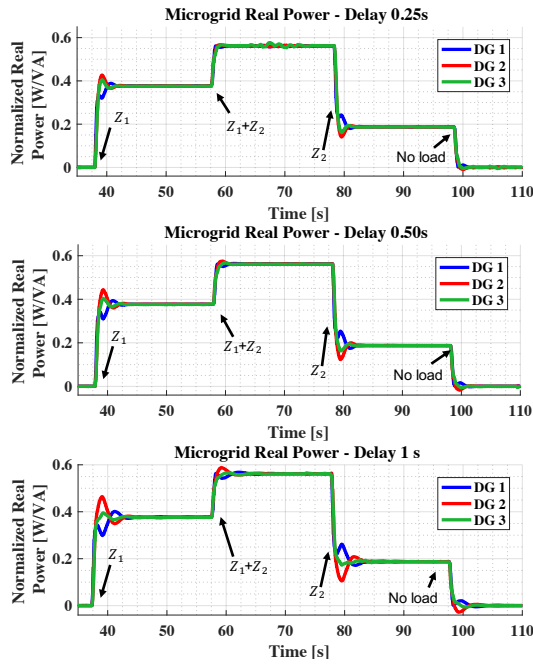


Fig. 12. Microgrid Behavior with Communication Delays- Real Power response- top: $\tau_{ij} = 0.25s$  middle: $\tau_{ij} = 0.5s$  bottom: $\tau_{ij} = 1s$

sating latency effects even beyond the prediction horizon.

## V. CONCLUSIONS AND FINAL REMARKS

In this paper, a distributed predictive controller was presented to regulate the frequency and average voltage and to achieve real and reactive power consensus in the microgrid. The main contribution of this paper is the proposed model used to solve the DMPC, which is based on droop, power transfer and phase angle equations. The proposed formulation includes explicit operational constraints to ensure operation of the microgrid within feasible ranges, and it is able to modify its adjacency matrix according to either electrical or communications disturbances.

The experimental results showed that the proposed controller has good performance against electrical disturbances such as load changes or disconnection/reconnection of DGs. Additionally, a good microgrid performance was achieved against communication issues such as latency and data packet losses.

Finally, as future work, the application of this type of DMPC to hybrid AC/DC microgrids with energy storage systems is suggested.

## ACKNOWLEDGMENT

Juan S. Gómez has been supported by a Ph.D. scholarship from the CONICYT-PCHA/Doctorado Nacional para extranjeros/2015- 21150555. This study was partially supported by the FONDECYT 1170683 grant, Complex Engineering Systems Institute (CONICYT – PIA – FB0816), Solar Energy Research Center SERC-Chile (CONICYT/FONDAP/Project under Grant 15110019) and the NSERC Discovery Grant RGPIN- 2017-04008.

## REFERENCES

- [1] R. Patton, C. Kambhampati, A. Casavola, P. Zhang, S. Ding, and D. Sauter, "A Generic Strategy for Fault-Tolerance in Control Systems Distributed Over a Network," *European Journal of Control*, vol. 13, no. 2-3, pp. 280–296, jan 2007.
- [2] M. Tucci and G. Ferrari-Trecate, "A scalable line-independent design algorithm for voltage and frequency control in AC islanded microgrids," *CoRR*, vol. abs/1703.02336, 2017.
- [3] S. Rivero, F. Sarzo, and G. Ferrari-Trecate, "Plug-and-Play Voltage and Frequency Control of Islanded Microgrids With Meshed Topology," *IEEE Transactions on Smart Grid*, vol. 6, no. 3, pp. 1176–1184, may 2015.
- [4] R. Olfati-Saber, J. A. Fax, and R. M. Murray, "Consensus and Cooperation in Networked Multi-Agent Systems," *Proceedings of the IEEE*, vol. 95, no. 1, pp. 215–233, jan 2007.
- [5] F. Bullo, "Lectures on Network Systems," in *Lectures on Network Systems*, 2018, ch. 4, pp. 47–61, with contributions by J. Cortes, F. Dorfler, and S. Martinez.
- [6] J. W. Simpson-Porco, Q. Shafiee, F. Dorfler, J. C. Vasquez, J. M. Guerrero, and F. Bullo, "Secondary Frequency and Voltage Control of Islanded Microgrids via Distributed Averaging," *IEEE Transactions on Industrial Electronics*, vol. 62, no. 11, pp. 7025–7038, nov 2015.
- [7] L. Zhang, H. Gao, and O. Kaynak, "Network-Induced Constraints in Networked Control Systems—A Survey," *IEEE Transactions on Industrial Informatics*, vol. 9, no. 1, pp. 403–416, feb 2013.
- [8] Y.-B. Zhao, X.-M. Sun, J. Zhang, and P. Shi, "Networked Control Systems: The Communication Basics and Control Methodologies," *Mathematical Problems in Engineering*, vol. 2015, pp. 1–9, 2015.
- [9] C. Ahumada, R. Cardenas, D. Saez, and J. M. Guerrero, "Secondary Control Strategies for Frequency Restoration in Islanded Microgrids With Consideration of Communication Delays," *IEEE Transactions on Smart Grid*, vol. 7, no. 3, pp. 1430–1441, may 2016.
- [10] S. Liu, X. Wang, and P. X. Liu, "Impact of Communication Delays on Secondary Frequency Control in an Islanded Microgrid," *IEEE Transactions on Industrial Electronics*, vol. 62, no. 4, pp. 2021–2031, apr 2015.
- [11] Y. Xu, H. Sun, W. Gu, Y. Xu, and Z. Li, "Optimal Distributed Control for Secondary Frequency and Voltage Regulation in an Islanded Microgrid," *IEEE Transactions on Industrial Informatics*, vol. 3203, no. c, pp. 1–1, 2018.
- [12] G. Chen and Z. Guo, "Distributed Secondary and Optimal Active Power Sharing Control for Islanded Microgrids with Communication Delays," *IEEE Transactions on Smart Grid*, vol. 3053, no. c, pp. 1–1, 2017.
- [13] L. Liang, Y. Hou, and D. J. Hill, "Design guidelines for MPC-based frequency regulation for islanded microgrids with storage, voltage, and ramping constraints," *IET Renewable Power Generation*, vol. 11, no. 8, pp. 1200–1210, jun 2017.
- [14] Y. Zhang, L. Fu, W. Zhu, X. Bao, and C. Liu, "Robust model predictive control for optimal energy management of island microgrids with uncertainties," *Energy*, vol. 164, pp. 1229–1241, dec 2018.
- [15] L. G. Marín, N. Cruz, D. Sáez, M. Sumner, and A. Núñez, "Prediction interval methodology based on fuzzy numbers and its extension to fuzzy systems and neural networks," *Expert Systems with Applications*, vol. 119, pp. 128–141, apr 2019.
- [16] M. H. Andishgar, E. Gholipour, and R. Allah Hooshmand, "An overview of control approaches of inverter-based microgrids in islanding mode of operation," pp. 1043–1060, dec 2017.
- [17] D. E. Olivares, A. Mehrizi-Sani, A. H. Etemadi, C. A. Canizares, R. Irvani, M. Kazerani, A. H. Hajimiragha, O. Gomis-Bellmunt, M. Saeedifard, R. Palma-Behnke, G. A. Jimenez-Estevéz, and N. D. Hatziargyriou, "Trends in Microgrid Control," *IEEE Transactions on Smart Grid*, vol. 5, no. 4, pp. 1905–1919, jul 2014.
- [18] P. Sina, "State of the art in research on Microgrids," *IEEE Access*, vol. 3, no. 1, pp. 890–925, 2015.
- [19] P. D. Christofides, R. Scattolini, D. Muñoz de la Peña, and J. Liu, "Distributed model predictive control: A tutorial review and future research directions," *Computers & Chemical Engineering*, vol. 51, pp. 21–41, apr 2013. [Online]. Available: <https://linkinghub.elsevier.com/retrieve/pii/S0098135412001573>
- [20] E. F. Camacho and C. Bordons, "Constrained Model Predictive Control," in *Model Predictive control*, 2nd ed., ser. Advanced Textbooks in Control and Signal Processing. London: Springer London, 2007, no. december, ch. 7, pp. 177–216.
- [21] R. M. Hermans, A. Jokić, M. Lazar, A. Alessio, P. P. van den Bosch, I. A. Hiskens, and A. Bemporad, "Assessment of non-centralised model

- predictive control techniques for electrical power networks,” *International Journal of Control*, vol. 85, no. 8, pp. 1162–1177, aug 2012.
- [22] G. Lou, W. Gu, W. Sheng, X. Song, and F. Gao, “Distributed Model Predictive Secondary Voltage Control of Islanded Microgrids With Feedback Linearization,” *IEEE Access*, vol. 6, pp. 50 169–50 178, 2018.
- [23] A. J. Babqi and A. H. Etemadi, “MPC-based microgrid control with supplementary fault current limitation and smooth transition mechanisms,” *IET Generation, Transmission & Distribution*, vol. 11, no. 9, pp. 2164–2172, jun 2017.
- [24] D. Clarke and R. Scattolini, “Constrained receding-horizon predictive control,” *IEE Proceedings D Control Theory and Applications*, vol. 138, no. 4, p. 347, 1991.
- [25] B. Kouvaritakis and M. Cannon, “MPC with No Model Uncertainty,” in *Model Predictive Control*, ser. Advanced Textbooks in Control and Signal Processing. Cham: Springer International Publishing, 2016, ch. 2, pp. 13–64.
- [26] C. Schmid and L. Biegler, “Quadratic programming methods for reduced hessian SQP,” *Computers & Chemical Engineering*, vol. 18, no. 9, pp. 817–832, sep 1994.
- [27] F. Bullo, “Lectures on Network Systems,” in *Lectures on Network Systems*, 2018, ch. 2, pp. 15–28, with contributions by J. Cortes, F. Dorfler, and S. Martinez.
- [28] —, “Lectures on Network Systems,” in *Lectures on Network Systems*, 2018, ch. 10, pp. 167–179, with contributions by J. Cortes, F. Dorfler, and S. Martinez.